Measurement of $\bar{p}p$ and pp Elastic Scattering in the Dip Region at $\sqrt{s} = 53$ GeV

A. Breakstone,[(1),(a)] H. B. Crawley,[(1)] G. M. Dallavalle,[(5)] K. Doroba,[(6)] D. Drijard,[(3)] F. Fabbri,[(3)] A. Firestone,[(1)] H. G. Fischer,[(3)] H. Frehse,[(3),(b)] W. Geist,[(3),(c)] G. Giacomelli,[(2)] R. Gokieli,[(6)] M. Gorbics,[(1)] P. Hanke,[(5)] M. Heiden,[(3),(c)] W. Herr,[(5)] E. E. Kluge,[(5)] J. W. Lamsa,[(1)] T. Lohse,[(4)] W. T. Meyer,[(1)] G. Mornacchi,[(3)] T. Nakada,[(5),(d)] M. Panter,[(3)] A. Putzer,[(5)] K. Rauschnabel,[(4)] F. Rimondi,[(2)] G. P. Siroli,[(2)] R. Sosnowski,[(6)] M. Szczekowski,[(3)] O. Ullaland,[(3)] and D. Wegener[(4)]

[(1)] *Ames Laboratory and Iowa State University, Ames, Iowa 50011*

[(2)] *Dipartimento di Fisica dell'Università and Istituto Nazionale di Fisica Nucleare, Bologna, Italy*

[(3)] *CERN, European Organization for Nuclear Research, Geneva, Switzerland*

[(4)] *Institut für Physik der Universität, Dortmund, Germany*

[(5)] *Institut für Hochenergiephysik der Universität, Heidelberg, Germany*

[(6)] *University and Institute for Nuclear Studies, Warsaw, Poland*

(Received 1 February 1985)

We have measured the differential cross section for $\bar{p}p$ and pp elastic scattering at $\sqrt{s} = 53$ GeV in the interval $0.5 < |t| < 4.0$ $(\text{GeV}/c)^2$ at the CERN intersecting storage rings using the split-field magnet detector. The shape of the differential cross section differs significantly between $\bar{p}p$ and pp scattering in the region $1.1 < |t| < 1.5$ $(\text{GeV}/c)^2$, with $\bar{p}p$ data showing a less pronounced dip structure than pp data.

PACS numbers: 13.85.Dz

Knowledge of the differential cross sections for $\bar{p}p$ and pp elastic scattering is of fundamental importance in the understanding of hadronic interaction dynamics. In particular, a difference between the $\bar{p}p$ and pp cross sections in the dip region [four-momentum transfer squared around 1.4 $(\text{GeV}/c)^2$] may indicate the presence of terms in the elastic scattering amplitude which are odd under crossing symmetry. The recent measurement of the $\bar{p}p$ elastic differential cross section at the CERN superconducting proton synchrotron collider by Bozzo *et al.*[1] added interest to this question because it showed no dip structure. Several theoretical models[2–9] used to explain the structure at collider energies have widely varying predictions for the shape of the $\bar{p}p$ differential cross section at intersecting storage-rings (ISR) energies. Thus we have extended our previous measurements of elastic $\bar{p}p$ and pp scattering[10] to higher values of the four-momentum transfer squared, t, which required higher $\bar{p}p$ luminosities than had been achieved previously at the ISR.

Shortly before the decommissioning of the ISR, a final $\bar{p}p$ run was made. With good performance of the antiproton accumulator and the ISR, an average luminosity of 3×10^{27} $\text{cm}^{-2}\,\text{s}^{-1}$ in our intersection region was achieved for a three week period, yielding a total integrated luminosity of 2.9×10^{33} cm^{-2}. Short comparison runs with pp collisions at a luminosity of 10^{30} $\text{cm}^{-2}\,\text{s}^{-1}$ were made before and after the $\bar{p}p$ run, allowing us to minimize systematic errors in the comparison of $\bar{p}p$ and pp elastic scattering. The integrated luminosity for the pp data was 1.5×10^{34} cm^{-2}. We used the split-field magnet (SFM) detector[11] with a two-stage elastic trigger described in our previous work.[10] Approximately 4×10^6 elastic triggers each for $\bar{p}p$ and pp were collected, 90% of which were taken with a modification to the basic trigger to reject elastic events with $|t| < 0.4$ $(\text{GeV}/c)^2$.

The analysis of the data was done in three steps. First, the data were passed through a fast filter program to reject most of the events with $|t| < 0.46$ $(\text{GeV}/c)^2$. Approximately 40% of the events remained after the filter. These were reconstructed with the standard SFM track-finding and -fitting program. Events were kept only if exactly one track with the appropriate charge was found near the outgoing beam line on each side with a reconstructed momentum close to the nominal beam momentum. This selection step rejected all but 30 000 (120 000) $\bar{p}p$ (pp) events. Finally, to determine more precisely t and ϕ (the azimuthal angle in the center-of-mass system), the surviving events were refitted requiring the magnitudes of the momenta of the outgoing tracks to be equal to the beam momenta. After fitting, the t resolution, $\Delta t/t$, was found to decrease with increasing $|t|$ from 5% at $|t| = 0.5$ $(\text{GeV}/c)^2$ to 2% at $|t| = 3.0$ $(\text{GeV}/c)^2$. The t and ϕ values for each track were then calculated and compared. For elastic events in the final sample, we required the two tracks to have t values differing by less than 0.2 $(\text{GeV}/c)^2$ and ϕ values collinear to 10°.

The acceptance of the apparatus, including the trigger efficiency, was determined by simulating the detector response to generated elastic events. These simulated events were passed through a trigger simulation followed by the same reconstruction chain as used for the data. For events with $|t| < 1.0$ $(\text{GeV}/c)^2$, only those events within ϕ regions of high acceptance were used. The statistical precision of the data would not al-

TABLE I. Values of $d\sigma/dt$ in mb/(GeV/c)^2. Quoted errors include statistical and point-to-point uncertainties arising from the corrections. The systematic scale error is estimated to be $\pm 30\%$ for $\bar{p}p$ and $\pm 20\%$ for pp data.

	pp			$\bar{p}p$		
$\lvert t \rvert$ range (Gev/c)^2	$\lvert t \rvert$ (GeV/c)^2	Number of events	$d\sigma/dt$ mb/(Gev/c)^2	$\lvert t \rvert$ (GeV/c)^2	Number of events	$d\sigma/dt$ mb/(GeV/c)^2
0.50 - 0.55				0.523	475	$(1.79 \pm 0.13) \times 10^{-1}$
0.55 - 0.60				0.570	225	$(8.55 \pm 0.73) \times 10^{-2}$
0.60 - 0.65	0.623	3240	$(6.33 \pm 0.36) \times 10^{-2}$	0.625	139	$(3.37 \pm 0.74) \times 10^{-2}$
0.65 - 0.70	0.673	2103	$(4.12 \pm 0.24) \times 10^{-2}$	0.674	98	$(2.35 \pm 0.53) \times 10^{-2}$
0.70 - 0.75	0.722	1509	$(2.39 \pm 0.08) \times 10^{-2}$	0.721	118	$(2.04 \pm 0.22) \times 10^{-2}$
0.75 - 0.80	0.772	906	$(1.45 \pm 0.06) \times 10^{-2}$	0.772	68	$(1.19 \pm 0.16) \times 10^{-2}$
0.80 - 0.85	0.823	510	$(8.48 \pm 0.42) \times 10^{-3}$	0.822	45	$(7.13 \pm 1.13) \times 10^{-3}$
0.85 - 0.90	0.873	436	$(4.53 \pm 0.24) \times 10^{-3}$	0.875	178	$(4.79 \pm 0.44) \times 10^{-3}$
0.90 - 0.95	0.924	266	$(2.71 \pm 0.18) \times 10^{-3}$	0.924	102	$(2.63 \pm 0.30) \times 10^{-3}$
0.95 - 1.00	0.974	159	$(1.65 \pm 0.14) \times 10^{-3}$	0.973	53	$(1.45 \pm 0.23) \times 10^{-3}$
1.00 - 1.05	1.023	177	$(5.91 \pm 0.75) \times 10^{-4}$	1.021	39	$(6.67 \pm 1.27) \times 10^{-4}$
1.05 - 1.10	1.074	104	$(3.47 \pm 0.49) \times 10^{-4}$	1.075	38	$(6.52 \pm 1.25) \times 10^{-4}$
1.10 - 1.15	1.124	65	$(2.16 \pm 0.35) \times 10^{-4}$	1.125	28	$(4.81 \pm 1.03) \times 10^{-4}$
1.15 - 1.20	1.173	27	$(8.90 \pm 1.94) \times 10^{-5}$	1.171	18	$(3.08 \pm 0.79) \times 10^{-4}$
1.20 - 1.30	1.243	37	$(6.10 \pm 1.18) \times 10^{-5}$	1.25	11	$(9.4 \pm 3.0) \times 10^{-5}$
1.30 - 1.40	1.349	13	$(2.13 \pm 0.63) \times 10^{-5}$	1.34	9	$(7.7 \pm 2.7) \times 10^{-5}$
1.40 - 1.50	1.460	17	$(2.79 \pm 0.73) \times 10^{-5}$	1.44	7	$(6.0 \pm 2.4) \times 10^{-5}$
1.50 - 1.60	1.546	19	$(3.14 \pm 0.79 \times 10^{-5}$	1.57	6	$(5.1 \pm 2.2) \times 10^{-5}$
1.60 - 1.70	1.650	19	$(3.13 \pm 0.79) \times 10^{-5}$	1.66	5	$(4.2 \pm 1.9) \times 10^{-5}$
1.70 - 1.80	1.753	24	$(3.96 \pm 0.90) \times 10^{-5}$	1.75	8	$(6.9 \pm 2.5) \times 10^{-5}$
1.80 - 1.90	1.844	28	$(4.65 \pm 1.00) \times 10^{-5}$	1.85	9	$(7.7 \pm 2.7) \times 10^{-5}$
1.90 - 2.00	1.952	28	$(4.61 \pm 0.99) \times 10^{-5}$	1.93	6	$(5.1 \pm 2.2) \times 10^{-5}$
2.00 - 2.10	2.059	27	$(4.47 \pm 0.97) \times 10^{-5}$			
2.10 - 2.20	2.148	32	$(5.30 \pm 1.08) \times 10^{-5}$			
2.00 - 2.20				2.09	12	$(5.1 \pm 1.6) \times 10^{-5}$
2.20 - 2.30	2.24	12	$(1.98 \pm 0.61) \times 10^{-5}$			
2.30 - 2.40	2.35	10	$(1.64 \pm 0.55) \times 10^{-5}$			
2.20 - 2.40				2.27	8	$(3.4 \pm 1.2) \times 10^{-5}$
2.40 - 2.50	2.45	12	$(1.98 \pm 0.61) \times 10^{-5}$			
2.50 - 2.60	2.54	13	$(2.13 \pm 0.63) \times 10^{-5}$			
2.40 - 2.60				2.48	3	$(1.3 \pm 0.7) \times 10^{-5}$
2.60 - 2.70	2.64	10	$(1.64 \pm 0.55) \times 10^{-5}$			
2.70 - 2.90	2.81	7	$(5.7 \pm 2.2) \times 10^{-6}$			
2.60 - 3.00				2.82	3	$(6.3 \pm 3.7) \times 10^{-6}$
2.90 - 3.10	2.99	13	$(1.06 \pm 0.31) \times 10^{-5}$			
3.10 - 3.30	3.24	7	$(5.7 \pm 2.2) \times 10^{-6}$			
3.00 - 4.00				3.52	2	$(1.7 \pm 1.2) \times 10^{-6}$
3.30 - 3.50	3.39	4	$(3.3 \pm 1.7) \times 10^{-6}$			

low this procedure to be used for $|t| > 1.0$ (GeV/c)^2. Instead, we used an average acceptance of 45% given by the Monte Carlo event simulation. We determined independently from the Monte Carlo calculation and by comparing the pp data to previous measurements[12] that the acceptance correction is constant in t to $\pm 10\%$ for $|t| > 1.0$ (GeV/c)^2. We also corrected the data for nuclear absorption, which amounted to a 12% correction, independent of t, in our t range. Multiple Coulomb scattering is negligible in our apparatus in this t range. In addition, we simulated the background process, $\bar{p}p \rightarrow \bar{p}p\pi^0$ with the π^0 undetected, and determined it to be of negligible importance after the cuts requiring t and ϕ matching of the two tracks. After all cuts we were left with 1713 elastic scattering events from the $\bar{p}p$ and 9834 for the pp data sets which were used for the differential-cross-section calculations. The normalizations were determined by requiring that the differential cross sections smoothly match onto those of our previous experiment.[10] Including the error in this matching, we estimate the uncertainty in the absolute normalization to be $\pm 30\%$ for the $\bar{p}p$ cross section and $\pm 20\%$ for the pp cross section. The relative normalization uncertainty between our $\bar{p}p$ and pp differential cross sections is $\pm 20\%$.

The measured differential cross sections are given in Table I and Figs. 1 (pp) and 2 ($\bar{p}p$). The t values given in the table are the average values from the data in a

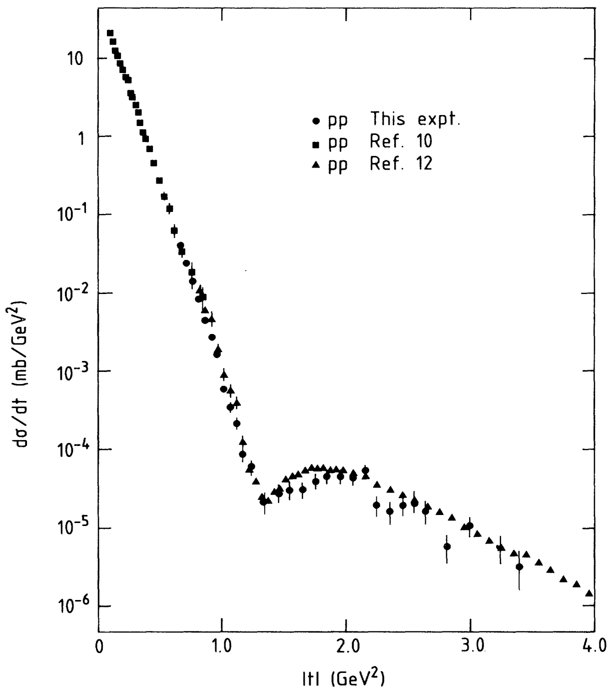

FIG. 1. Elastic differential pp cross section at $\sqrt{s} = 53$ GeV. Only t-dependent errors are shown. The systematic scale error is estimated at $\pm 20\%$. Included are the low-t data from our previous experiment (Ref. 10) and the pp data of Ref. 12.

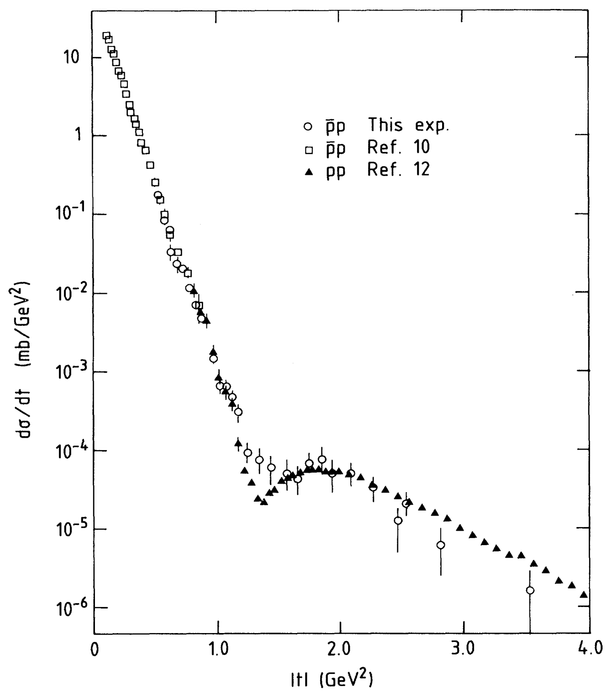

FIG. 2. Elastic differential $\bar{p}p$ cross section at $\sqrt{s} = 53$ GeV. Only t-dependent errors are shown. The systematic scale error is estimated at $\pm 30\%$. Included are the low-t data from our previous experiment (Ref. 10) and the pp data of Ref. 12.

given t bin. The systematic error on the t scale is less than 0.004 $(\mathrm{GeV}/c)^2$ for both the $\bar{p}p$ and pp data. To check for consistency with our previous measurements,[10] we made simple exponential fits of the form $d\sigma/dt = a\exp(bt)$ in the range $0.5 < |t| < 1.0$ $(\mathrm{GeV}/c)^2$ [$0.6 < |t| < 1.0$ $(\mathrm{GeV}/c)^2$] for $\bar{p}p$ (pp), yielding slope values which are consistent with, but less accurate than, our previous measurements.[10]

The comparison of our pp differential cross section for $|t| > 0.8$ $(\mathrm{GeV}/c)^2$ to a more precise experiment[12] shows good agreement of the shapes of the two data sets (Fig. 1); however, there is a normalization difference of 30%, which is within the normalization uncertainties of the two experiments. On the other hand, the $\bar{p}p$ data (Fig. 2) show a different structure in the dip region. This is well illustrated in Fig. 3, where we show the ratio of our $\bar{p}p$ data to the pp data of Ref. 12 multiplied by the relative normalization factor of 0.71. Based on a simple χ^2 calculation, the hypothesis that the $\bar{p}p$ and pp cross sections are equal (i.e., the ratio is 1) in the region $1.1 < |t| < 1.5$ $(\mathrm{GeV}/c)^2$ can be excluded to the 99.9% confidence level (χ^2/d.o.f. $=21/5$).

When we compare the available models to these data we find that none of them describes the data adequately. In particular, when comparing to the models which fit the data of Bozzo *et al.* and make quantitative predictions for our energy we find the following: (1) The model of Bourrely, Soffer, and Wu[3] predicts a pronounced dip at $|t| = 1.2$ $(\mathrm{GeV}/c)^2$ which is not observed in the data, (2) the model of Donnachie and Landshoff[7] provides a shape that is in reasonable agreement with the data but that is significantly too high in magnitude, and (3) the nucleon valence core model of Islam, Fearnley and Guillaud[9] predicts a sharp dip at $|t| = 1.0$ $(\mathrm{GeV}/c)^2$ and is in strong disagreement with these data.

In conclusion, we report the first detailed measurement of the differential elastic scattering cross section for $\bar{p}p$ in the dip region at $\sqrt{s} = 53$ GeV. A comparison to the pp differential cross section shows a significantly different structure in the dip region. This is in contrast to another recent experiment at this same energy[13] which, based on much fewer events, found no statistically significant difference between the pp and $\bar{p}p$ data.

We are grateful for the support provided by the SFM detector group and the ISR Experimental Support group. We also thank R. Messerli and U. Gruhn for their cooperation. This work was supported in part by the U. S. Department of Energy and in part by a grant from the Bundesministerium für Wissenschaft und

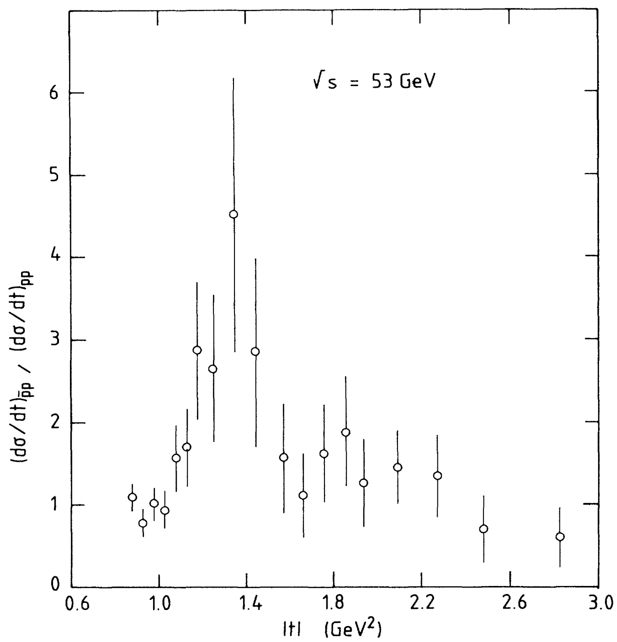

FIG. 3. The ratio of the $\bar{p}p$ differential cross section from this experiment to the pp differential cross section of Ref. 12 in the range $0.7 < |t| < 3.0$ $(\mathrm{GeV}/c)^2$. The pp data of Ref. 12 have been multiplied by the factor 0.71 to take into account the normalization differences of the two experiments. Only t-dependent errors are shown. The ratio has an overall uncertainty of $\pm 30\%$ due to these normalization uncertainties.

Forschung of the Federal Republic of Germany.

[a]Present address: Department of Physics, University of Hawaii, Honolulu, Haw. 96822.

[b]Present address: CDC, Zürich, Switzerland.

[c]Present address: Lawrence Berkeley Laboratory, Berkeley, Cal. 94720.

[d]Present address: Swiss Institute for Nuclear Research, Villigen, Switzerland.

[1]M. Bozzo *et al.*, in *Proceedings of the Fourteenth International Symposium on Multiparticle Dynamics, Lake Tahoe, Nevada, 1983,* edited by J. F. Gunion and P. H. Yager (World Scientific, Singapore, 1984).

[2]A. J. Buras and J. Dias de Deus, Nucl. Phys. **B71**, 481 (1974).

[3]C. Bourrely, J. Soffer, and T. T. Wu, Phys. Rev. D **19**, 3249 (1979), and Phys. Lett. **121B**, 284 (1983), and Phys. Rev. Lett. **54**, 757 (1985).

[4]H. Cheng, J. K. Walker, and T. T. Wu, Phys. Lett. **44B**, 97 (1973).

[5]T. T. Chou and C. N. Yang, Phys. Rev. Lett. **46**, 764 (1981), and Phys. Lett. **128B**, 457 (1983).

[6]J. Dias de Deus and P. Kroll, J. Phys. G **9**, L81 (1983).

[7]A. Donnachie and P. V. Landshoff, Phys. Lett. **123B**, 345 (1983), and Nucl. Phys. **B231**, 189 (1984).

[8]G. W. Heines and M. M. Islam, Nuovo Cimento **61A**, 149 (1981).

[9]M. M. Islam, T. Fearnley, and J. P. Guillaud, Nuovo Cimento **81A**, 737 (1984).

[10]A. Breakstone *et al.*, Nucl. Phys. **B248**, 253 (1984).

[11]W. Bell *et al.*, Nucl. Instrum. Methods **124**, 437 (1975), and Nucl. Instrum. Methods **156**, 111 (1978).

[12]E. Nagy *et al.*, Nucl. Phys. **B150**, 221 (1979).

[13]S. Erhan *et al.*, CERN Report No. EP/84-147, 1984 (to be published).